Journal of Archaeological Science 52 (2014) 428–435

Contents lists available at ScienceDirect

Journal of Archaeological Science

journal homepage: http://www.elsevier.com/locate/jas

Unreliability of the induced obsidian hydration method with abbreviated hot-soak protocols

Alexander K. Rogers [a, *], Daron Duke [b]

[a] Archaeology Curator, Maturango Museum, United States
[b] Far Western Anthropological Research Group, Inc., United States

ARTICLE INFO

Article history:
Received 14 May 2014
Received in revised form
28 August 2014
Accepted 8 September 2014
Available online 28 September 2014

Keywords:
OHD
Obsidian
Hydration
Induced hydration

ABSTRACT

The induced hydration method is based on temperature scaling; obsidian samples are hydrated in the laboratory at elevated temperatures, and hydration rims are then measured. The activation energy and diffusion constant are determined analytically, and the hydration rate computed for temperatures of archaeological interest. It is desirable to minimize the hot-soak times in the interest of efficient use of laboratory equipment; however, the technique yields poor results for some obsidians when used with such experimental protocols. We applied the induced hydration method to obsidian specimens from seven sources in southeastern Nevada, using a frequently-used protocol which minimizes the hot-soak times. We then measured the hydration rims using optical microscopy. When plotted graphically, the resulting rates are not linear as would be expected, but instead consistently form shallow sigmoid curves. They are also found to be unrealistically high. Further, we find that hydration rate varies with time at a constant temperature, contrary to expectations. We conclude that this protocol does not adequately model long-term hydration and discuss the implications of this finding. We recommend the development of experimental designs that adequately model long-term hydration.

1. Introduction

Obsidian hydration as a technique for constructing archaeological chronologies dates from the 1960 article by Friedman and Smith (1960). Since that time, the technique of obsidian hydration dating (OHD) has gone through periods of great enthusiasm (e.g., Friedman and Long, 1976; Hull, 2001; Rogers, 2007, 2012) and periods of rejection and disillusionment (e.g., Ridings, 1995). Nevertheless, it is a widely used technique in the archaeology of the American desert west, where frequently no other data exist for constructing a chronology.

Quantitative measurement of hydration rate by induced hydration is part of this equivocal history for OHD in archaeology. The temperature dependence of hydration rate is well known, and attempts have been made in the past to measure hydration rate in the laboratory (e.g., Friedman and Long, 1976; Michels et al., 1983a,1984; Stevenson and Scheetz, 1989; Stevenson et al., 1998). However, rates measured in the laboratory often do not agree well with archaeological data (see, for example, the pointed observations in Hall and Jackson, 1989:32) and are generally not trusted by practicing archaeologists today. The method has, however, recently been demonstrated to yield results which are consistent with archaeological data in the case of Topaz Mountain obsidian from Utah (Rogers and Duke, 2011) and obsidians on Rapa Nui, Chile (Stevenson et al., 2013).

This paper describes an analysis in which the induced hydration technique, with hydration measured by optical microscopy, was employed with obsidian specimens from seven sources in southeastern Nevada; the research was carried out under the Lincoln County Archaeological Initiative (LCAI), a Bureau of Land Management (BLM)-administered program to support archaeological research in Lincoln County, Nevada. The experimental protocol was developed in consonance with Origer's Obsidian Laboratory, to yield readable hydration rims and still minimize the hot-soak times. Minimizing hot-soak times is desirable because longer hot-soak times tend to tie up laboratory assets and reduce throughput. However, the computed rates do not conform to theoretical expectations: they are found to form a shallow sigmoid curve instead of a straight line when plotted in the form of the logarithmic Arrhenius equation, and to be unrealistically high. Since the sigmoid is consistent across specimens and sources, it is unlikely to be due to random errors.

* Corresponding author. Tel.: +1 760 375 6900.
E-mail addresses: matmus1@maturango.org, akrogers1@verizon.net (A.K. Rogers).

http://dx.doi.org/10.1016/j.jas.2014.09.007
0305-4403/

A further experiment was thus conducted with the obsidians by measuring the hydration rate over extended hot-soak times, which indicated a variation in hydration rates with time at a constant temperature, which is also contrary to the Arrhenius model. Other researchers have observed a similar effect when measured by Secondary Ion Mass Spectrometry (Anovitz et al., 2004; Stevenson and Novak, 2011) or by water mass uptake (Stevenson and Novak, 2011), but this seems to be the first time it has been observed with optical microscopy.

We conclude that, in order for the induced hydration process to yield valid hydration rates at archaeological temperatures, the measurements must be made after sufficient time for the process to be past the transient phase and reach equilibrium. We recommend that any researcher using induced hydration review the rate development procedure, and determine that near equilibrium conditions were reached.

2. Hydration measurement techniques

Obsidian is an alumino-silicate, or rhyolitic, glass that is formed by rapid cooling of magma under the proper geologic conditions. Like any other glass, it is not a crystal, and thus it lacks the lattice structure typical of crystals at the atomic level. Glasses do, however, possess a matrix-like structure exhibiting some degree of spatial order (Doremus, 1994:27, Fig. 2; 2002:59–73). Obsidians are typically about 75% SiO_2 and about 20% Al_2O_3 by weight, the remainder being source-specific trace elements (Doremus, 2002:109, Table 8.1; Stevenson et al., 1998). The minute interstices within the glass matrix, on the order of 0.1–0.2 nm in diameter, are where water diffusion takes place. All obsidians also contain small amounts of water, known as intrinsic water or structural water, resulting from the magma formation process; the amount is generally <2% by weight, although cases of somewhat higher concentration are occasionally encountered.

Glass is often viewed as an inert material, easy to clean and not subject to corrosion, but this is not true at the molecular level. Glass, including obsidian, is readily eroded by water, especially deionized water at high temperature and pressure (Stevenson et al., 1998).

Three methodologies have been reported in the literature for measuring obsidian hydration. The first is measurement of water mass increase or loss vs. time (Ebert et al., 1991; Newman et al., 1986; Stevenson and Novak, 2011). This is based on the knowledge that the process of water mass increase is a function of temperature, pressure, and openness of the glass matrix as measured by intrinsic water concentration. Water mass gain or loss proceeds proportional to t^n where t is time and n is an exponent lying between approximately 0.5 and 0.6 (Stevenson and Novak, 2011).

A second method is direct measurement of water profiles vs. depth (Anovitz et al., 1999, 2004, 2008; Riciputi et al., 2002; Stevenson et al., 2004). The water concentration profile measurement is generally performed by Secondary Ion Mass Spectrometry (SIMS) or the electron microprobe, using H+ ions as a proxy for water. The principle is to measure the concentration of H^+ ions as a function of depth into the obsidian. The depth of the half-amplitude point is found to be proportional to t^n, where t is time and n is an exponent lying between approximately 0.6 and 0.7 (Anovitz et al., 1999, 2004; Stevenson and Novak, 2011).

The third method is to measure the width of the hydration rim by observation of the leading edge of the hydrated zone, or the stress region, from the artifact edge by polarized optical microscopy (many papers, e.g., Friedman and Smith, 1960; Friedman and Long, 1976). The stress arises because the volume hydrated volume has enlarged due to penetration of the glass matrix by water molecules, while the matrix of the unhydrated glass has not. Measurement in classic OHD is by optical microscopy, using a polarized microscope at a magnification of at least 500X. This is the most widely used obsidian hydration dating technique in archaeology today due to its low cost and apparent simplicity. All experimental evidence, and correlation with archaeological data, indicate that the position of this stress zone, or hydration front, progresses into the obsidian proportional to t^n, where n is approximately 0.5 within limits of experimental error (Rogers and Duke, 2011; Stevenson and Scheetz, 1989; Stevenson et al., 1998). The agreement with classic diffusion theory, in particular Fick's formulations and the Boltzmann transformation (Crank, 1975:105ff.; Rogers, 2007, 2012), may be a coincidence or may be due to an as-yet-undiscovered property of the diffusion process itself. Because of the popularity of this technique, it is the basis of the analysis reported here.

3. Principles of induced hydration

The induced hydration method (Anovitz et al., 2004; Michels et al., 1983, 1984; Rogers and Duke, 2011; Stevenson and Scheetz, 1989; Stevenson et al., 1998, 2004) is based on temperature scaling, with the key assumption that the functional form of the temperature dependence is known (the so-called Arrhenius model, discussed below). Obsidian samples are hydrated in the laboratory at five elevated temperatures between 110 °C and 150 °C, using silicon-buffered distilled water to eliminate the possibility of surface erosion of the specimens. The protocol typically terminates the hot-soak times once a clearly measureable hydration rim has developed, and hydration rims are then measured. The activation energy and diffusion constant are determined analytically, and hydration rate is computed from the Arrhenius model for a temperature of archaeological interest (20 °C in this case). The mathematical technique for computing activation energy and pre-exponential factor (or diffusion constant) is based on methods developed in physical chemistry for computing reaction kinetics (Cvetanovic et al., 1979). Table 1 summarizes five previously-employed laboratory protocols, with the protocol employed in this paper.

Obsidian hydration is by definition a time-dependent phenomenon, as the amount of water absorbed by the glass increases with time. Regardless of measurement method, an implicit assumption is that the hydration rate is constant with time at any

Table 1
Typical experimental protocols employed in induced hydration studies.

Obsidian	Temperature range, °C	Hot-soak time range, days	Number of temperature-time combinations per specimen	Reference
East Africa	150–200	0.5–4	9	Michels et al., 1983b
Camels Back Cave, UT	150–200	0.5–4	9	Michels 1984
Coso volcanic field CA	160–190	3–12	4	Stevenson and Scheetz 1989
Camels Back Cave, UT	110–150	29–58	3	Rogers and Duke 2011
Seven various	150–190	40–60	4–6	Stevenson and Novak 2011
Lincoln County, NV	110–150	10–30	4–6	This paper

given temperature; when this occurs the process is in equilibrium. A further implicit assumption in the induced hydration protocol is that the hydration process reaches equilibrium within a small fraction of the hot-soak time, so that the majority of hydration occurs at a constant rate. If this condition is not met, the Arrhenius model is not valid and the induced hydration method gives incorrect rates.

Stevenson and Rogers (2014) report that equilibrium is probably not reached with the hot-soak times typically employed. Their data showed that water cross-sectional densities in the hydrated layer decrease with temperature, whereas Henry's law, which describes equilibrium conditions, would predict a water density increase. They conclude that use of measurements after short-term hot-soak may result in unrepresentative values of activation energy and, hence, incorrect hydration rates. The results of the present analysis bear this out.

4. Analytical technique

The basic equation for progression of the optical hydration front into the obsidian is.

$$r^2 = Dt \tag{1}$$

where r is the hydration rim thickness, D is the diffusion coefficient, and t is time; units of D are typically μ^2/yr (Doremus, 2002). The diffusion coefficient D is a function of temperature by the Arrhenius equation

$$D = A\exp(-E/T) \tag{2}$$

where A is the diffusion constant or "pre-exponential," E is activation energy in °K, and T is temperature in °K (Doremus, 2002; Rogers, 2007). Note that D is a function of temperature, but E and A are not, and also that D is constant at any given temperature.

Finally, combining Equations (1) and (2) and expressing in logarithmic form yields the so-called logarithmic Arrhenius equation.

$$\ln\left(r^2/t\right) = \ln(A) - E/T \tag{3}$$

If we define $y = \ln(r^2/t)$ and $x = 1/T$, Equation (4) becomes a linear equation of the form.

$$y = I + Sx \tag{4}$$

with $I = \ln(A)$ and $S = -E$. Given data for r, t, and T for two or more points, Equations (3) and (4) can be solved as a linear best fit (Cvetanovic et al., 1979; Meyer, 1975):

$$S = \left\{\sum w_i \sum w_i x_i y_i - \sum w_i x_i \sum w_i y_i\right\}/D \tag{5a}$$

$$I = \left\{\sum w_i x_i^2 \sum w_i y_i - \sum w_i x_i \sum w_i x_i y_i\right\}/D \tag{5b}$$

and

$$D = \sum w_i \sum w_i x_i^2 - \left(\sum w_i x_i\right)^2 \tag{5c}$$

Finally, the slope value S is the negative of the activation energy E, and A, the diffusion constant, is given by.

$$A = \exp(I) \tag{6}$$

The parameter w_i in Equation (5a–c) is the weight factor for each data point, given by $w_i = 1/\sigma_i^2$, where σ_i^2 is the variance in the y-dimension associated with the ith data point (Cvetanovic et al., 1979). For the functional form $y = \ln(r^2/t)$ it can be shown by the theory of propagation of errors that appropriate weight factors are given by $w_i = 1/((2CV_r)^2 + CV_t^2)$, where CV_r and CV_t are the coefficients of variation for r and t respectively (Cvetanovic et al., 1979; Taylor 1982:179ff.).

For this analysis, the value of CV_r is computed from the hydration rim values provided by the laboratory, which exhibit a standard deviation of 0.085 μ. The value of CV_t is estimated from laboratory procedures by assuming that the hot-soak time might vary from an exact number of days by up to an hour or so, or about 0.05 days. The standard deviation of the uncertainty is then $0.05/\sqrt{(12)}$, which is then used in computing CV_t.

A final source of experimental error lies in the temperature controller for the laboratory oven used for the hot soak. Typical laboratory thermostat controllers are accurate to about ±1 °C. It can be shown, in terms of effective hydration temperature, that this adds a temperature increment of 0.06 °C to the nominal temperature of the controller. This was taken into account in the analysis process.

The linear best fit in Equation (5a–c) provides best estimates for the mean values of activation energy (E), diffusion constant or pre-exponential (A), and hydration rate. Uncertainties associated with these mean values are characterized by the standard deviations of the activation energy and diffusion constant, which are, respectively,

$$\sigma_E = \sigma\left\{\sum w_i / D\right\} \tag{7}$$

and

$$\sigma_A = A\sigma\left\{\sum w_i x_i^2 / D\right\} \tag{8}$$

with D defined in Equation (6c) and σ given by

$$\sigma = \left\{\sum w_i (y_i - \hat{y}_i)^2 / (N-2)\right\}^{1/2} \tag{9}$$

Here x_i and y_i are defined as above, $\hat{y}$ is the best-fit value of y_i computed from Equation (5a–c), and N is the number of data points. The parameter σ is known as the "external or *a posteriori* standard deviation" (Cvetanovic et al., 1979:52).

Computation of the errors in hydration rate is more complicated. It cannot be simply inferred from σ_E and σ_A, because there is also a cross-correlation term contributing to the error. To avoid this complexity, the standard deviation of the rate was computed by a Monte Carlo simulation in MatLab, using the observed uncertainties in r, t and T (Rogers, 2006).

5. Data set and analysis

The data set for Lincoln County consists of 21 specimens from seven geochemical sources, each hydrated at five different temperatures (110 °C, 120 °C, 130 °C, 140 °C, 150 °C). Higher

Table 2
Nevada obsidian sources and specimens.

Source	Number of specimens
Timpahute Range	1
Meadow Valley Mountains	3
Delamar Mountains	6
Panaca Summit	6
Clover Mountains	2
Wilson Creek Range	2
South Pahroc	1

Table 3
Induced hydration data on Lincoln County obsidian specimens.

Cat. No.	ID	JOB#	XRF source	*t*, days	*T*, deg C	Rim mean, μ	Rim std. dev, μ
H03-28-2	13	R-90	Timpahute Range	30	110	1.92	0.08
	27	R-91	Timpahute Range	25	120	2.07	0.08
	41	R-92	Timpahute Range	20	130	2.45	0.08
	55	R-94	Timpahute Range	15	140	2.97	0.12
	69	R-95	Timpahute Range	10	150	3.07	0.05
H12-1	1	R-90	Meadow Valley Mountains	30	110	2.05	0.08
	15	R-91	Meadow Valley Mountains	25	120	2.38	0.08
	29	R-92	Meadow Valley Mountains	20	130	2.98	0.08
	43	R-94	Meadow Valley Mountains	15	140	3.60	0.06
	57	R-95	Meadow Valley Mountains	10	150	3.67	0.12
H12-2	2	R-90	Meadow Valley Mountains	30	110	2.02	0.10
	16	R-91	Meadow Valley Mountains	25	120	2.42	0.08
	30	R-92	Meadow Valley Mountains	20	130	2.93	0.05
	44	R-94	Meadow Valley Mountains	15	140	3.53	0.05
	58	R-95	Meadow Valley Mountains	10	150	3.53	0.08
H12-3	3	R-90	Meadow Valley Mountains	30	110	2.02	0.04
	17	R-91	Meadow Valley Mountains	25	120	2.32	0.12
	31	R-92	Meadow Valley Mountains	20	130	2.92	0.12
	45	R-94	Meadow Valley Mountains	15	140	3.52	0.04
	59	R-95	Meadow Valley Mountains	10	150	3.60	0.06
H12-4	4	R-90	Delamar Mountains	30	110	2.75	0.05
	18	R-91	Delamar Mountains	25	120	2.98	0.10
	32	R-92	Delamar Mountains	20	130	3.72	0.08
	46	R-94	Delamar Mountains	15	140	4.50	0.11
	60	R-95	Delamar Mountains	10	150	4.82	0.10
	78	R-100	Delamar Mountains	10	150	4.83	0.05
H12-4F	71	R-100	Delamar Mountains	10	150	3.67[a]	0.08
H12-5	5	R-90	Delamar Mountains	30	110	1.90	0.09
	19	R-91	Delamar Mountains	25	120	2.50	0.09
	33	R-92	Delamar Mountains	20	130	3.02	0.10
	47	R-94	Delamar Mountains	15	140	3.68	0.04
	61	R-95	Delamar Mountains	10	150	3.53	0.05
	79	R-100	Delamar Mountains	10	150	3.73	0.08
H12-5A	72	R-100	Delamar Mountains	10	150	3.57	0.05
H12-5B	73	R-100	Delamar Mountains	10	150	3.68	0.04
H12-5C	74	R-100	Delamar Mountains	10	150	3.57	0.08
H12-6	6	R-90	Panaca Summit	30	110	1.97	0.05
	20	R-91	Panaca Summit	25	120	2.53	0.08
	34	R-92	Panaca Summit	20	130	2.95	0.08
	48	R-94	Panaca Summit	15	140	3.57	0.05
	62	R-95	Panaca Summit	10	150	3.67	0.10
H12-7	7	R-90	Panaca Summit	30	110	2.72	0.10
	21	R-91	Panaca Summit	25	120	3.07	0.08
	35	R-92	Panaca Summit	20	130	3.73	0.08
	49	R-94	Panaca Summit	15	140	4.52	0.10
	63	R-95	Panaca Summit	10	150	4.90	0.13
	80	R-100	Panaca Summit	10	150	4.85	0.05
H12-7A	75	R-100	Panaca Summit	10	150	3.08[a]	0.08
H12-7B	76	R-100	Panaca Summit	10	150	2.95[a]	0.08
H12-7C	77	R-100	Panaca Summit	10	150	3.25[a]	0.05
H12-8	8	R-90	Panaca Summit	30	110	2.05	0.05
	22	R-91	Panaca Summit	25	120	2.40	0.09
	36	R-92	Panaca Summit	20	130	2.97	0.08
	50	R-94	Panaca Summit	15	140	3.50	0.01
	64	R-95	Panaca Summit	10	150	3.50	0.11
H12-9	9	R-90	Clover Mountains	30	110	1.68	0.04
	23	R-91	Clover Mountains	25	120	1.98	0.08
	37	R-92	Clover Mountains	20	130	2.58	0.08
	51	R-94	Clover Mountains	15	140	3.18	0.10
	65	R-95	Clover Mountains	10	150	3.00	0.13
H12-10	10	R-90	Clover Mountains	30	110	1.77	0.10
	24	R-91	Clover Mountains	25	120	2.07	0.12
	38	R-92	Clover Mountains	20	130	2.68	0.12
	52	R-94	Clover Mountains	15	140	3.00	0.09
	66	R-95	Clover Mountains	10	150	3.10	0.13
H12-11	11	R-90	Wilson Creek Range	30	110	1.72	0.10
	25	R-91	Wilson Creek Range	25	120	1.92	0.10
	39	R-92	Wilson Creek Range	20	130	2.60	0.11
	53	R-94	Wilson Creek Range	15	140	3.07	0.08
	67	R-95	Wilson Creek Range	10	150	3.17	0.08
S. Pahroc	12	R-90	South Pahroc Range	30	110	1.83	0.08
	26	R-91	South Pahroc Range	25	120	2.10	0.11
	40	R-92	South Pahroc Range	20	130	2.50	0.09
	54	R-94	South Pahroc Range	15	140	3.02	0.08

(*continued on next page*)

Table 3 (*continued*)

Cat. No.	ID	JOB#	XRF source	*t*, days	*T*, deg C	Rim mean, μ	Rim std. dev, μ
	68	R-95	South Pahroc Range	10	150	3.30	0.13
Wilson Crk	14	R-90	Wilson Creek Range	30	110	1.82	0.04
	28	R-91	Wilson Creek Range	25	120	1.95	0.05
	42	R-92	Wilson Creek Range	20	130	2.67	0.05
	56	R-94	Wilson Creek Range	15	140	3.07	0.05
	70	R-95	Wilson Creek Range	10	150	3.17	0.08

[a] Anomalous readings from supplementary specimens. Not included in computations.

temperatures are avoided as they often lead to diffuse hydration rims. The experiment was performed by Tom Origer, Origer's Obsidian Laboratory, using a protocol in which the hot-soak times were terminated once a clearly measureable hydration rim had developed (30, 25, 20, 15, 10 days, respectively). Hydration was performed in liquid phase using distilled water buffered with dissolved silicon dioxide to inhibit surface erosion. The hydration bands were measured with a strainfree 60-power objective and a Bausch and Lomb 12.5-power filar micrometer eyepiece mounted on a Nikon Labophot-Pol polarizing microscope, and each hydration rim value represents an average of six individual readings. Table 2 summarizes the obsidian sources, as named by Richard Hughes, Geochemical Research Laboratory, and the number of specimens.

The data analyzed are in Table 3. In each case, a catalog number (Cat. No.) refers to a sequence of temperature runs conducted on flakes from a given obsidian specimen from a given geologic sampling locale. In cases such as Cat. No. H12-4F, the flake is from the same geochemical source as H12-4, but from a different piece of obsidian.

The data in Table 3 were analyzed by the linear best fit technique described above, with the standard deviation of the rate computed by Monte Carlo simulation. Table 4 summarizes the results by individual catalog numbers.

6. Discussion

Table 5 shows the induced hydration rates summarized by geochemical source; *N* is the number of catalog numbers applying to each source.

To cross-check the hydration rates, the results for the three most commonly used obsidian sources in the region—Meadow Valley Mountains, Delamar Mountains, and Panaca Summit—were computed based on time-diagnostic projectile points collected archaeologically. Rates were computed based on dating by temporally sensitive artifacts and by associated radiocarbon samples; Rogers and Duke (2014) give the details of the computation and the data sets used. The rate for Meadow Valley Mountains obsidian is 12.79 μ^2/1000 yrs, for Delamar Mountains is 18.32 μ^2/1000 yrs, and for Panaca Summit is 15.25 μ^2/1000 yrs μ^2/1000 yrs—all at 20 °C. These rates have been shown to yield archaeologically reasonable ages when tested on field data from sites in the Moapa Valley, Nevada (Rogers and Duke, 2014). Clearly none of the induced hydration strategies yields a rate that agrees with the archaeologically derived rates (Table 6). Also shown is the ratio of the archaeological rate to the induced rate.

To address these discrepancies, an analysis of errors was conducted, focusing on the three sources for which archaeological rates had been computed. Plotting the induced hydration data in the logarithmic Arrhenius form (Equation (4)), shows an unexpected phenomenon: the data do not lie on a straight line as the model predicts, but instead exhibit a slight sigmoid shape. Fig. 1 shows typical behavior, and the Lincoln County data set exhibits this consistently across all specimens. Since it is consistent, it is clearly not caused by random errors in the laboratory. Adjusting the value of the exponent of the rim value *r* in Equation (1) changes the overall slope of the line, but does not affect the sigmoid shape.

It has long been understood that application of the linear best fit process to analysis of induced hydration data is very sensitive to experimental errors (see discussion in Rogers, 2006). In brief, the sensitivity arises from two sources, the first being the extrapolation process implied in Equation (4): solving Equation (4) for the value of the intercept I involves extrapolating the best-fit line beyond the range of data, which amplifies errors. The second error source lies in the mathematical form of Equation (6), since computing the diffusion constant A requires raising the extrapolated value I to an exponential, which further amplifies errors. However, these factors should lead to random errors rather than to the systematic variation seen here.

Another implication of the sigmoid shape of the logarithmic Arrhenius plots is that the computed hydration rates vary systematically as data points are excluded. Table 7 shows the three archaeologically evaluated cases with their rates computed with all five temperatures, their rates computed with the 110 °C data point eliminated, and their rates computed with only the three central data points (120 °C, 130 °C, 140 °C).

Two points can be observed here. First, we observed that the ratio of archaeological rate to induced rate with this protocol is very consistent for these sources (0.54 ± 0.03). The differences are not statistically distinguishable. The reason for this close similarity is not known.

Second, the data set is statistically fragile, as exclusion of a single data point causes a significant change in the outcome. With the exception of specimen 12–5, the computed hydration rates decrease monotonically as data points are deleted. This is indicative of the presence of systematic effect, as random errors would not cause this.

The divergence between induced hydration rates and archaeological rates may lie in the material properties of obsidian. A slight relaxation has been found to occur in the surface layer of the obsidian as hydration progresses, which affects the measured value of hydration rate (Anovitz et al., 2004). Stevenson and Novak (2011:1721) made high-precision measurements of hydration rate in Napa Glass Mountain obsidian by Secondary Ion Mass Spectrometry (SIMS) at a temperature of 90 °C. Progress of the hydration was measured by the depth of the full-width/half-maximum (FWHM, or 50%) point in the SIMS trace of H^+ concentration vs. depth. They noted that the value of $FWHM^2/t$, which represents the classic definition of hydration rate, first increases and then decreases over time. Fig. 2 is a plot of their data showing the variation over time (Stevenson and Novak, 2011).

In the case of Lincoln County obsidian, optical microscopy was used to measure glass deformation resulting from the relaxation noted by Anovitz et al. (2004). Since SIMS is an order of magnitude more precise than optical microscopy, we performed an experiment to verify the observability of this effect. Two specimens of Meadow Valley Mountains obsidian (H12-1 and H12-3) were hydrated at 140 °C, and hydration rims were read optically at 15, 30,

Table 4
Lincoln County obsidian hydration rates.

Cat. No.	Obsidian source	Rate, μ^2/1000 yrs @ 20 °C		Activation energy, J °K/mole		Diffusion constant, μ^2/1000 yrs		N
		Mean	Std. dev	Mean	Std. Dev.	Mean	Std. dev.	
H03-28-2	Timpahute Range	33.80	12.48	73,063	4648	3.53E+11	4.84E+11	5
H12-1	Meadow Valley Mtns	22.78	7.30	79,407	3459	3.22E+12	3.27E+12	5
H12-2	Meadow Valley Mtns	28.68	9.26	77,079	3284	1.56E+12	1.51E+12	5
H12-3	Meadow Valley Mtns	21.41	6.98	79,565	3550	3.23E+12	3.38E+12	5
H12-4	Delamar Mtns	34.64	7.70	80,072	3567	6.42E+12	6.68E+12	6
H12-5	Delamar Mtns	29.22	7.60	77,129	3234	1.62E+12	1.51E+12	9
H12-6	Panaca Summit	23.89	7.59	78,983	2469	2.83E+12	2.06E+12	5
H12-7	Panaca Summit	32.74	7.23	80,679	2918	7.77E+12	6.62E+12	6
H12-8	Panaca Summit	33.91	10.97	75,591	3226	1.00E+12	9.52E+11	5
H12-9	Clover Mtns	15.86	6.04	79,748	7017	2.57E+12	5.32E+12	5
H12-9	Clover Mtns	15.86	6.04	79,748	7017	2.57E+12	5.32E+12	5
H12-10	Clover Mtns	23.61	8.79	76,431	3159	9.83E+11	9.16E+11	5
H12-11	Wilson Creek Range	11.96	4.59	82,217	4648	5.34E+12	7.31E+12	5
Wilson Creek	Wilson Creek Range	18.37	6.90	78,734	5096	1.97E+12	2.96E+12	5

Table 5
Induced Hydration Rates for Nevada Obsidians. Hydration Rate in μ^2/1000 yrs @ 20 °C.

Obsidian source	Mean rate	Rate SD	CV	*N*
Meadow Valley Mountains	24.29	8.52	0.35	3
Delamar Mountains	31.93	8.12	0.25	2
Panaca Summit	30.18	9.84	0.33	3
Clover Mountains	19.74	8.48	0.43	2
Wilson Creek Range	15.17	6.68	0.44	2
Timpahute Range	33.80	12.48	0.37	1
South Pahroc Range	16.15	5.99	0.37	1

Table 6
Comparison of Induced and Archaeological Hydration Rates, in μ^2/1000 yrs @ 20 °C.

Obsidian source	Induced rate	Archaeological rate	Ratio
Meadow Valley Mountains	24.29	12.79	0.53
Delamar Mountains	31.93	18.32	0.57
Panaca Summits	30.18	15.25	0.51

45, and 60 days. The first run, H12-3, was terminated at 45 days due to laboratory error; the other ran the full 60 days. Fig. 3 shows the results for specimen 12-1; the data for 12-3 at 15, 30, and 45 days are virtually identical.

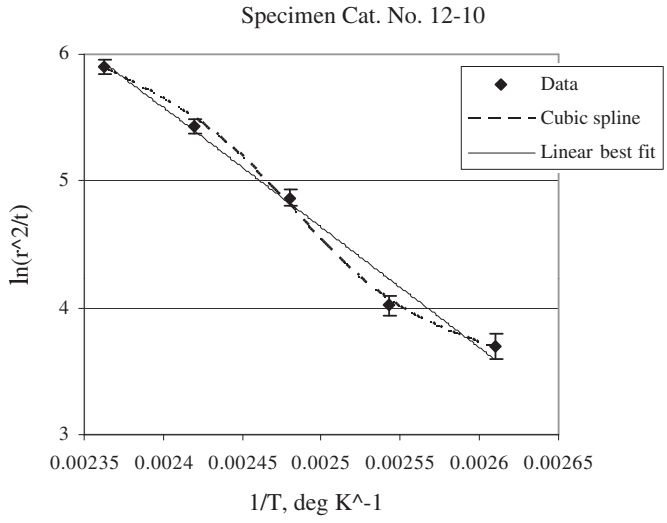

Fig. 1. Logarithmic Arrhenius plot for Wilson Creek Range obsidian, specimen 12-10, showing sigmoid shape. Other specimens are similar. Spline added to guide the eye.

Table 7
Hydration rates for Lincoln County Obsidians, μ^2/1000 yrs at 20 °C.

Cat. No.	Source	All data points	110 °C point deleted	3 central points only
H03-28-2	Timpahute Range	33.80	14.81	9.04
H12-1	Meadow Valley Mtns	22.78	12.18	6.50
H12-2	Meadow Valley Mtns	28.68	26.01	10.05
H12-3	Meadow Valley Mtns	21.41	14.97	5.85
H12-4	Delamar Mtns	34.64	16.24	10.86
H12-5	Delamar Mtns	29.22	41.41	9.25
H12-6	Panaca Summit	23.89	27.01	17.47
H12-7	Panaca Summit	32.74	17.99	14.52
H12-8	Panaca Summit	33.91	29.28	11.18

The profound implication of our results is that the hydration rate is not constant with time for these hydration conditions. An inspection of Figs. 2 and 3 suggests that the transient decay time is a function of temperature, proceeding more rapidly at higher temperatures. Fig. 3 shows that the rate does not approach equilibrium until times greater than about 60 days for Meadow Valley Mountains obsidian at 140 °C; by contrast, the measurements reported in Table 3 at 140 °C were made after a time of only 15 days, long before

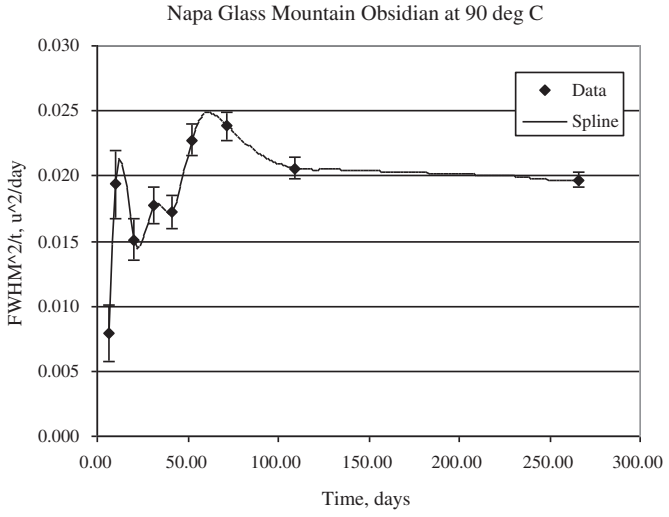

Fig. 2. Induced hydration rate for Napa Glass Mountain obsidian, hydrated at 90 °C, showing variation over time. Full-width half-maximum point (FWHM) measured by SIMS. Error bars based on assumed 0.03 μ error in SIMS readings. Spline added to guide the eye. Data from.Stevenson and Novak (2011)

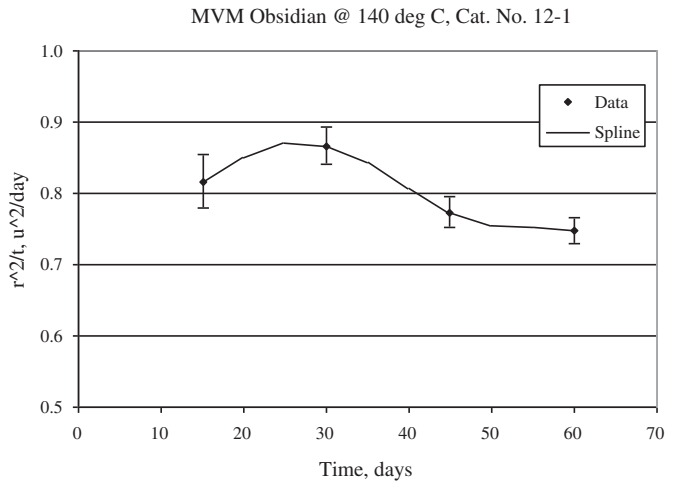

Fig. 3. Variation of hydration rate with time for Meadow Valley Mountains obsidian, specimen 12-1. Spline added to guide the eye.

the hydration process reached equilibrium. Thus the hydration rims are being measured during the non-equilibrium period, and a complicated interaction between temperature and time is probably producing the observed sigmoid. Moreover, since the measurements are being before equilibrium is reached, they are unlikely to result in valid estimates of the equilibrium values of activation energy or hydration rate.

It is known that the viscosity of obsidian decreases with increasing intrinsic water content and with increasing temperature (Friedman et al., 1963); it is also known that the hydration rate increases with increasing intrinsic water content (Zhang, 1991; Zhang and Behrens, 2000). The relaxation phenomenon which causes the stress region is due to water molecules within the glass matrix and is resisted by the viscosity of the glass. Thus, increasing temperature should lead to a more rapid approach to equilibrium, which seems to be true here.

Plotting the induced hydration data from Stevenson and Scheetz (1989) in logarithmic Arrhenius form bears this out. Fig. 4 shows the plots for two obsidian sources from the Coso volcanic field in eastern California, West Sugarloaf (WSL) and Sugarloaf Mountain (SLM), with differing intrinsic water. Obsidian from the SLM source has higher intrinsic water content than WSL concentrations (1.02 vs. 0.62 wt%, respectively) and a correspondingly higher hydration rate (Rogers, 2008; Stevenson et al., 1993). Fig. 4 shows that the sigmoid for SLM is less pronounced than for WSL, suggesting that the lower viscosity of SLM obsidian is allowing a more rapid approach to equilibrium conditions. Similar sigmoid behavior is also evident in data published on east African obsidians by Michels et al. (1983b).

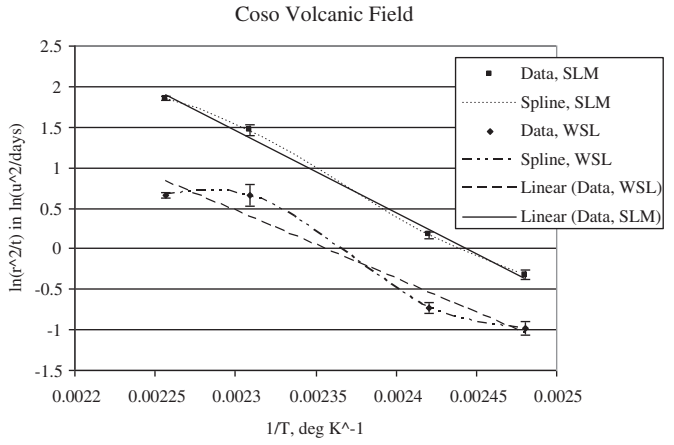

Fig. 4. Logarithmic Arrhenius plots for obsidians from the Coso volcanic field, Inyo County, California. SLM = Sugarloaf Mountain, WSL = West Sugarloaf. Splines added to guide the eye.

The transient behavior observed above therefore appears to result from an interaction between water diffusion and mechanical relaxation of the glass, in which the two phenomena proceed with comparable rates. This corresponds to the "anomalous diffusion" case described by Crank (1975:254–255), and places the hydration process midway between "glassy polymers" and "rubbery polymers" (Crank, 1975:254–255). An initial analysis has shown that polymer diffusion models yield a good fit to water penetration data (Rogers and Stevenson, 2014), but the details of such a model have not yet been developed.

7. Conclusions

The experiment reported here was performed using a protocol in which the hot-soak times were terminated once a clearly measureable hydration rim had developed. The induced hydration rates resulting from this experiment do not conform to theoretical expectations in three respects. First, when plotted in the form of the logarithmic Arrhenius equation, the data should form a straight line, but instead form a shallow sigmoid curve. Because the deviation is consistent across 21 specimens from seven different obsidian sources, this pattern is unlikely to be due to random errors but rather a heretofore-unobserved property of the obsidian.

Second, the induced hydration rates are found to vary systematically as data points are excluded, which would not occur if the deviation were due to random errors. Inclusion of all five data points results in unrealistically high rates, while use of only the three central points results in rates which are too low; exclusion of a single end point results in rates which fall between the two extremes. However, none of the rates computed from induced hydration agrees well with rates determined from archaeological data, usually resulting in ages that are too young.

Third, hydration rate measured at a single temperature (140 °C) shows the rate is initially not constant over time, as the Arrhenius model assumes. Similar phenomena have been observed by other investigators using other techniques (Anovitz et al., 2004; Stevenson and Novak, 2011). Such variation with time at a constant temperature invalidates the basic Arrhenius model of the hydration rate in the context of a rapid experimental protocol, which is the theoretical basis of the induced hydration methodology.

The use of the Arrhenius model with a rapid-measurement protocol assumes the obsidian hydration process quickly reaches equilibrium. However, Stevenson and Rogers (2014) have reported measurements which suggest that equilibrium is not reached with the hot-soak times typically employed. The results of the present analysis support this conclusion. It is notable that Rogers and Duke (2011) developed induced a hydration rate for Camels Back Cave obsidian which agreed within 6% with an archaeologically derived rate; inspection of Table 1 shows that a relatively long hot-soak was employed. Stevenson et al. (2013) also achieved archaeologically consistent results with longer hot-soak times.

In order for the induced hydration process to yield valid hydration rates at archaeological temperatures, the measurements must be made after sufficient time for the process to be past the transient phase and reach equilibrium. This can be verified by making a series of measurements of hydration rate at constant temperature, similar to Fig. 3 above, and selecting hot-soak times

which are clearly in the equilibrium region. We recommend that any researcher using induced hydration review the rate development procedure, and determine that near equilibrium conditions were reached. Further, we recommend development of experimental designs that adequately model long term hydration.

Acknowledgments

This project was funded through the Lincoln County Archaeological Initiative with funds obtained through the sale of public lands administered by the BLM in Lincoln County, Nevada and approved under an inter-agency partnership authorized by the Lincoln County Land Act. We greatly appreciate the patience of Nick Pay, Kim Ferguson, and Carol Bass at the BLM as we moved through our experiments. We thank Tom Origer of Origer's Obsidian Laboratory for performing the laboratory measurements and Richard Hughes of Geochemical Research Laboratory for obsidian sourcing of the specimens and his assistance with their field collection. Heather Baron of Far Western provided crucial copy editing. We are grateful for many fruitful insights on obsidian hydration from Chris Stevenson of Virginia Commonwealth University. Finally, we thank two anonymous reviewers whose comments have greatly improved the quality of this paper. Any remaining errors are, of course, ours.

References

Anovitz, L.M., Elam, J.M., Riciputi, L.R., Cole, D.R., 1999. The failure of obsidian hydration dating: sources, implications, and new directions. J. Archaeol. Sci. 26 (7), 735–752.
Anovitz, L.M., Elam, J.M., Riciputi, L.R., Cole, D.R., 2004. Isothermal time-series determination of the rate of diffusion of water in Pachuca obsidian. Archaeometry 42 (2), 301–326.
Anovitz, Lawrence M., David, R. Cole, Mostafa, Fayek, 2008. Mechanisms of Rhyolitic Glass Hydration Below the Glass Transition. Am. Mineral 93, 1166–1178.
Crank, J., 1975. The Mathematics of Diffusion. Oxford University Press, Oxford.
Cvetanovic, R.J., Singleton, D.L., Paraskevopoulos, G., 1979. Evaluations of the mean values and standard errors of rate constants and their temperature coefficients. J. Phys. Chem. 83 (1), 50–60.
Doremus, R.H., 2002. Diffusion of Reactive Molecules in Solids and Melts. Wiley Interscience, New York.
Doremus, Robert H., 1994. Glass Science, second ed. Wiley-Interscience, New York.
Ebert, W.L., Hofburg, R.F., Bates, K.K., 1991. The Sorption of Water on Obsidian and a Nuclear Waste Glass. Phys. Chem. Glasses 32 (4), 133–137.
Friedman, Irving, Smith, R., 1960. A new method of dating using obsidian; part 1, the development of the method. Am. Antiq. 25, 476–522.
Friedman, Irving, Long, William, Smith, Robert L., 1963. Viscosity and water content of rhyolite glass. J. Geophys. Res. 68 (34), 6523–6535.
Friedman, Irving, Long, W.D., 1976. Hydration rate of obsidian. Science 191 (1), 347–352.
Hull, Kathleen L., 2001. Reasserting the utility of obsidian hydration dating: a temperature-dependent empirical approach to practical temporal resolution with archaeological obsidians. J. Archaeol. Sci. 28, 1025–1040.
Hall, Matthew C., Jackson, T.L., 1989. Obsidian hydration rates in California. Contributions of the University of California Archaeological Research Facility No. 48, Dec. 1989. In: Hughes, Richard C. (Ed.), Current Directions in California Obsidian Studies. University of California, Berkeley.
Meyer, Stuart, 1975. Data Analysis for Scientists and Engineers. Wiley, New York.
Michels, Joseph W., 1984. Hydration Rate Constants for Topaz Mountain Obsidian, Utah. MOHLAB Technical Report No. 34. State College, Pennsylvania.
Michels, J.W., Ignatius, S., Tsong, T., Smith, G.A., 1983a. Experimentally derived hydration rates in obsidian dating. Archaeometry 25, 107–117.
Michels, Joseph W., Ignatius, S., Tsong, T., Nelson, Charles M., 1983b. Obsidian dating and east African archaeology. Science 219, 361–363.
Newman, S., Stolper, E.M., Epstein, S., 1986. Measurement of Water in Rhyolitic Glasses: Calibration of an Infrared Spectroscopic Technique. Am. Mineral 71, 1527–1541.
Riciputi, Lee R., Elam, J.M., Anovitz, L.M., Cole, D.R., 2002. Obsidian diffusion dating by secondary ion mass spectrometry: a test using results from Mound 65, Clalco, Mexico. J. Archaeol. Sci. 29, 1055–1075.
Ridings, Rosanna, 1995. Where in the world does obsidian hydration dating work? Am. Antiq. 61 (1), 136–148.
Rogers, Alexander K., 2006. Induced hydration of obsidian: a simulation study of accuracy requirements. J. Archaeol. Sci. 33, 1696–1705.
Rogers, Alexander K., 2007. Effective hydration temperature of obsidian: a diffusion-theory analysis of time-dependent hydration rates. J. Archaeol. Sci. 34, 656–665.
Rogers, Alexander K., 2008. Obsidian hydration dating: accuracy and resolution limitations imposed by intrinsic water variability. J. Archaeol. Sci. 35, 2009–2016.
Rogers, Alexander K., 2012. Temperature correction for obsidian hydration dating. In: Liritzis, Ioannis, Stevenson, Christopher (Eds.), Obsidian and Ancient Manufactured Glasses. University of New Mexico Press, Albuquerque, pp. 46–56.
Rogers, Alexander K., Duke, Daron, 2011. An archaeologically validated protocol for computing obsidian hydration rates from laboratory data. J. Archaeol. Sci. 38, 1340–1345.
Rogers, Alexander K., Duke, Daron, 2014. Hydration Rates for Four Obsidians in Lincoln County, Nevada: Panaca Summit, Meadow Valley Mountains, Delamar Mountains, and Timpahute Range. Report prepared by Far Western Anthropological Research Group, Inc., for the BLM. Ely Field Office.
Rogers, Alexander K., Stevenson, Christopher M., 2014. Obsidian Hydration as "Diffusion-relaxation": a Polymer Model of the Hydration Process. Paper Presented at the Annual Meeting of the Society for American Archaeology. Texas, Austin.
Stevenson, Christopher M., Novak, Steven W., 2011. Obsidian hydration dating by infrared spectroscopy: method and calibration. J. Archaeol. Sci. 38, 1716–1726.
Stevenson, Christopher M., Rogers, Alexander K., 2014. Transient and equilibrium solubility of water in Rhyolytic Glass: Implications for hydration rate development at elevated temperature. J. Archaeol. Sci. 45, 15–19.
Stevenson, Christopher M., Scheetz, B.E., 1989. Induced hydration rate development of obsidians from the Coso volcanic field: a comparison of experimental procedures. In: Hughes, Richard E. (Ed.), Current Directions in California Obsidian Studies. Contributions of the University of California Archaeological Research Facility No. 48, Berkeley, pp. 23–30.
Stevenson, Christopher M., Knauss, E., Mazer, J.J., Bates, J.K., 1993. Homogeneity of water content in obsidian from the Coso volcanic Field: Implications for obsidian hydration dating. Geoarchaeology 8 (5), 371–384.
Stevenson, Christopher M., Mazer, J.J., Scheetz, B.E., 1998. Laboratory obsidian hydration rates: theory, method, and application. In: Shackley, M.S. (Ed.), Archaeological Obsidian Studies: Method and Theory. Advances in Archaeological and Museum Science, vol. 3. Plenum Press, New York, pp. 181–204.
Stevenson, Christopher M., Abdelrehim, I.M., Novak, Steven W., 2004. High precision measurement of obsidian hydration layers on artifacts from the Hopewell site using secondary ion mass spectrometry. Am. Antiq. 69 (4), 555–568.
Stevenson, Christopher M., Ladeford, Thegn N., Novak, Steven W., 2013. Prehistoric settlement chronology on rapa nui, Chile: obsidian hydration dating using infrared photoacoustic spectroscopy. J. Archaeol. Sci. 44, 3021–3030.
Taylor, John R., 1982. An Introduction to Error Analysis. University Science Books, Mill Valley.
Zhang, Youxue, Stolper, E.M., Wasserburg, G.J., 1991. Diffusion of water in rhyolitic glasses. Geochim. Cosmochim. Acta 55 (2), 441–456.
Zhang, Y., Behrens, H., 2000. H_2O diffusion in rhyolitic melts and glasses. Chem. Geol. 169, 243–262.